

Variable stars in the field of the open cluster NGC 7789 ¹

B. J. Mochejska¹ and J. Kaluzny^{1,2}

¹Warsaw University Observatory, Al. Ujazdowskie 4, PL-00-478 Warszawa, Poland

e-mail: mochejsk@sirius.astrow.edu.pl, jka@sirius.astrow.edu.pl

²Copernicus Astronomical Center, 00-716 Warszawa, Bartycka 18

ABSTRACT

We present the results of our search for variable stars in the intermediate-age open cluster NGC 7789. We have found 45 variable stars: 35 eclipsing binaries, five pulsating variables and five miscellaneous variables. Most of the eclipsing binaries show W UMa type of variability, with periods shorter than one day. Four systems exhibit unusual behavior: two, V4276 and V6698, are probably RS CVn stars, another, V3283, is a possible cataclysmic binary. The nature of the fourth binary, V2130, is unclear: the system exhibits asymmetric maxima. Among the pulsating variables two, V3407C and V4805 are background RR Lyrae stars and one, V6736, is a δ Scuti variable which is a blue straggler belonging to the cluster. Some of the miscellaneous variables may have periods longer than the five day timespan of our observations. We also present a color-magnitude diagram for the NGC 7789 open cluster, fairly complete down to $V \sim 20$. The relatively large number of variables found in the comparison field (14 compared to 31 in the cluster field) implies that objects not associated physically with the cluster can account for a significant number of variables identified in the cluster field, as well as in other globular and open clusters observed on a dense background/foreground of disk stars.

1. Introduction

We present the results of our search for variable stars in the rich intermediate-age open galactic cluster NGC 7789, located at $l = 115^{\circ}49, b = -5^{\circ}36$. The cluster has been the subject of only one previous search for variable stars, conducted by Jahn et al. (1995), which resulted in the discovery of 15 variables in the central part of the cluster.

The first extensive photometry of NGC 7789 was presented by Burbidge & Sandage (1958), providing magnitude and color determinations for nearly 700 stars within some $450''$ of the cluster center. Recent estimates place the age of the cluster at about 1.6 Gyr (Gim et al. 1998). A

¹Based on observations obtained at Kitt Peak National Observatory, a division of NOAO which is operated by the Association of Universities for Research in Astronomy, Inc. under cooperative agreement with the National Science Foundation.

determination of the distance modulus by Jahn et al. (1995) based on the lower limit of the red-giant clump on the color-magnitude diagram yields $(m - M)_V = 12.3$.

In section 2 we provide general information on the location of the monitored fields and the observations. Section 3 describes the reduction procedure applied to the collected data. In section 4 the method used for selecting candidate variables is discussed briefly. The color-magnitude diagrams are shown in Section 5. We present the catalog of variables in section 6. In section 7 we apply an absolute brightness calibration for contact binary systems to try to assess their cluster membership. A brief discussion of the results is presented in section 8.

2. Observations

The data for this project was obtained with the Kitt Peak National Observatory 0.9m telescope equipped with a Tektronix 2048×2048 CCD (T2KA camera) on five consecutive nights, from October 17 to 21, 1992. The field of view was about 23×23 arcmin² with the scale of $0.68''/pixel$.

Two fields were monitored, one centered on the NGC7789 open galactic cluster ($\alpha = 23^h 952$, $\delta = 56^\circ 71$). The other field, intended for comparison, was offset, for the most part, in right ascension and had a small overlap with the cluster field ($\alpha = 23^h 988$, $\delta = 56^\circ 64$).

Useful data was collected during five to six hours each night, except for the night of October 19, when only a few good frames were obtained, giving a total of 22.5 hours of monitoring. For the cluster field we obtained 68×420 sec and $9 \times 40 \div 90$ sec exposures in V , 5×600 sec and $4 \times 80 \div 120$ sec exposures in B . For the comparison field we collected 53×420 sec and $3 \times 60 \div 170$ sec exposures in V , 2×600 sec and one 120 sec exposure in B .

3. Data reduction

The preliminary processing of the CCD frames was done with the standard routines in the IRAF-CCDPROC package.² Due to imperfect mirror alignment stars on some parts of the frame had severely elongated point spread functions (PSF). In order not to deteriorate the quality of the photometry over the good parts of the frame the leftmost 500 columns were masked out with the IMREPLACE routine.

Photometry was extracted using the *Daophot/Allstar* package (Stetson 1987). A PSF varying quadratically with the position on the frame was used. Due to the large pixel scale, resulting in marginal sampling of stellar profiles, the PSF was modeled with a Gaussian function. Stars were

²IRAF is distributed by the National Optical Astronomy Observatories, which are operated by the Association of Universities for Research in Astronomy, Inc., under cooperative agreement with the NSF

identified using the FIND subroutine and aperture photometry was done on them with the PHOT subroutine. Around 150 bright isolated stars were initially chosen by *Daophot* for the construction of the PSF. Of those the stars with profile errors greater than twice the average were rejected and the PSF was recomputed. This procedure was repeated until no such stars were left on the list. The PSF was then further refined on frames with all but the PSF stars subtracted from them. This procedure was applied twice. The PSF obtained in the above method was then used by *Allstar* in profile photometry.

The frames intended as templates for our databases were taken as the average of three frames with the best seeing. A similar reduction procedure was applied as for single frames. After having obtained the profile photometry FIND was run again on the subtracted frame with a threshold of 10-15 sigma. Detections at a distance of less than one half FWHM from stars identified previously were rejected, as were the stars for which PHOT could not determine a magnitude. Upon closer examination the latter proved to be spurious peaks caused by the subtraction of the imperfect PSF, especially on the edges of the frames, where the PSF was deformed. Allstar was run again on the expanded list, which resulted in the rejection of some more objects, and then once more, to refine the positions of stars.

For many of the bright stars which were saturated on the template useful photometry could be obtained on most of the other images with inferior seeing. The brightest stars from a short exposure were selected and added to the template list. Great care was taken to remove false detections in the profiles of saturated stars from the final list.

The final template star list was then transformed to the (X, Y) coordinate system of each of the frames and used as input to *Allstar* in the fixed-position mode. The output profile photometry was transformed to the common instrumental system of the template image and then combined into a database. The databases were created for the 420 *sec* exposures in the *V* filter only in each of the two fields.

Equatorial coordinates were determined for all objects found on the *V* filter templates. The transformation from rectangular to equatorial coordinates was derived using 4045 and 3402 reference stars from the USNO-A2 catalog (Monet et al. 1996) for the cluster and the comparison field respectively. In both cases the average difference between the catalog and the computed coordinates was less than 0.5'' in right ascension and 0.25'' in declination.

4. Selection of variables

We have followed the procedure for selecting variables given in Kaluzny et al. (1998), where it is described in detail. Here, only a brief summary will be presented.

The reduction procedure described in the previous section produces databases of calibrated *V* magnitudes and their standard errors. The *V* databases for the cluster and the comparison fields

contained 10705 and 8143 stars, with up to 68 and 54 measurements, respectively.

Measurements flagged as “bad” (with unusually large *Daophot* errors, compared to other stars) and measurements with errors exceeding the average error, for a given star, by more than 4σ were removed. For further analysis we used only those stars that had at least $N_{good} > N_{max}/2$ measurements. There are 10153 and 7664 such stars in the *V* databases of the cluster and comparison fields, respectively.

Our next goal was to select a sample of variable stars from the total sample defined above. There are many ways to proceed, and we largely followed the approach of Stetson (1996), also described in Kaluzny et al.(1998). For each star we computed the Stetson’s variability index J_S and stars with values exceeding some minimum value $J_{S,min}$ were considered candidate variables. The definition of J_S is rooted in the assumption that on each visit to the program field at least one pair of observations is obtained, and only when both observations have a residual from the mean of the same sign does the pair contribute positively to the variability index. The definition of Stetson’s variability index includes the standard errors of individual observations. If, for some reason, these errors were over- or underestimated, we would either miss real variables, or select spurious variables as real ones. Using the procedure described in Kaluzny et al. (1998), we scaled the *Daophot* errors to better represent the “true” photometric errors. We then selected the candidate variable stars by computing the value of J_S for the stars in our *V* database. We used a cutoff of $J_{S,min} = 0.75$ to select 277 and 284 candidate variable stars in the cluster and the comparison fields, respectively.

The light curves of all variable candidates were examined, as were the images of the stars themselves on the CCD frames, to weed out false detections in the wings of bright stars, bad pixels, etc. After the rejection of spurious variables and stars with noisy/chaotic light curves we were left with 31 variables in the cluster field and 14 in the comparison field.

The periodicities for all candidate variables were analyzed using a variant of the Lafler-Kinman (1965) string-length technique proposed by Stetson (1996). The periods were then refined using the analysis of variance method, as described by Schwarzenberg-Czerny (1989).

5. Color-magnitude diagrams

To construct the color-magnitude diagrams we used the *V* photometry from the templates. To extend the CMD to lower magnitudes we added bright stars from our best quality short exposures. The *B* filter photometry for the cluster field was obtained from an image constructed from three long exposures with the best seeing, just as it was done for the *V* templates. Bright stars selected from a short *B* exposure were appended to the photometry list. In case of the comparison field only two long exposures in the *B* filter were available, taken far apart in time and under different seeing conditions. The photometry lists from the two images were merged, with the better of the two measurements retained for each star present on both lists. By better we mean the magnitude

determination with a smaller standard error, as computed by *Allstar*.

For the variable stars we have determined their V magnitudes and $B - V$ colors following a different procedure. In case of the eclipsing binaries we used the magnitude outside of the eclipses, V_{max} to position them on the CMD. For the pulsating stars we determined their average magnitude $\langle V \rangle$. The variables for which we did not derive a period were plotted with the maximum magnitude V_{max} they attained during our observing run.

To determine the colors of the variables the B magnitudes from the 600 sec. exposures were used. The V magnitudes were interpolated from two V exposures, one taken before and one after, to the beginning of the B exposure. The average $B - V$ colors were computed from four color determinations in the cluster field and two in the comparison field. The scatter of the color determinations for most variables brighter than 17th mag. was about 0.02 mag. Some of the eclipsing variables displayed a wider range of color variations, up to 0.2 mag., but that seems to be an intrinsic property of those systems, most likely caused by the different colors of the components of the detached systems or gravitational darkening in the semi-detached and contact pairs.

The transformation of the instrumental magnitudes to the standard system was derived from observations of the Landolt fields (Landolt 1992). The following relations were adopted:

$$\begin{aligned} v &= V - 0.002 \times (B - V) + const \\ b - v &= 0.966 \times (B - V) + const \end{aligned}$$

The zero points were determined from the unpublished photometry obtained by the second author on the KPNO 2.1m telescope in 1992.

The color-magnitude diagrams for the field centered on the cluster and the comparison field are shown in Figures 1 and 2, respectively. The diagram for the cluster field (Fig. 1) shows a well defined main sequence that can be traced down to $V \sim 20.5$ mag, and a substantial number of blue straggler candidates at its extension to lower magnitudes, as well as an extended red giant branch and a reasonably well-defined red clump. There is no obvious indication of a post main sequence gap. The comparison field CMD (Fig. 2) consists mainly of field stars, although the cluster main sequence is still discernible. We were able to trace it out easily to a distance of $\sim 15'$ from the cluster center. The depth of the CMDs is biased by the B band photometry. Figures 3 and 4 show the average standard V magnitude errors plotted as a function of V .

The color-magnitude diagram for the variable stars is presented in Figure 5. Each type of variables is denoted by a different symbol: eclipsing binaries by squares, pulsating variables by circles and miscellaneous by triangles. Stars within a radius of 500 pixels ($\sim 6'$) from the cluster center are plotted in the background. Solid symbols indicate cluster members confirmed by proper motion measurements (McNamara & Solomon 1981). The brightest and bluest variable, V9097, is a known non-member with 0% probability of belonging to the cluster. Variables located close (at less than about $6'$) to the center of the cluster show a tendency to group on and above the main sequence.

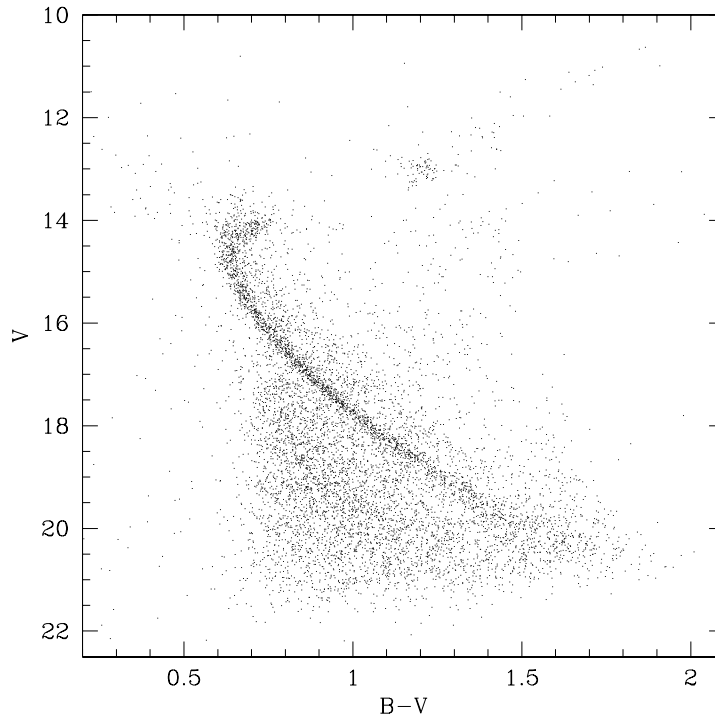


Fig. 1.— The color-magnitude diagram for the field centered on the NGC 7789 open cluster.

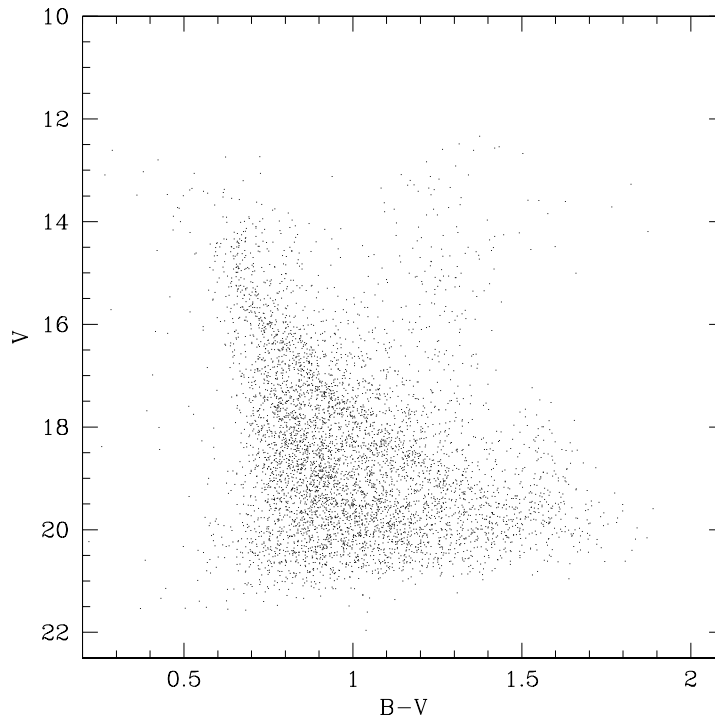


Fig. 2.— The color-magnitude diagram for the comparison field.

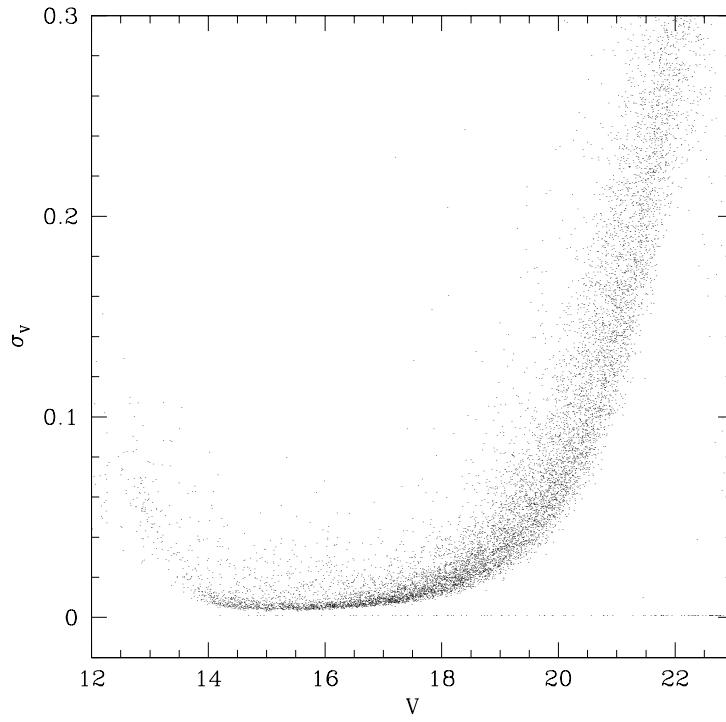


Fig. 3.— The average standard V magnitude errors plotted as a function of V for stars in the cluster field.

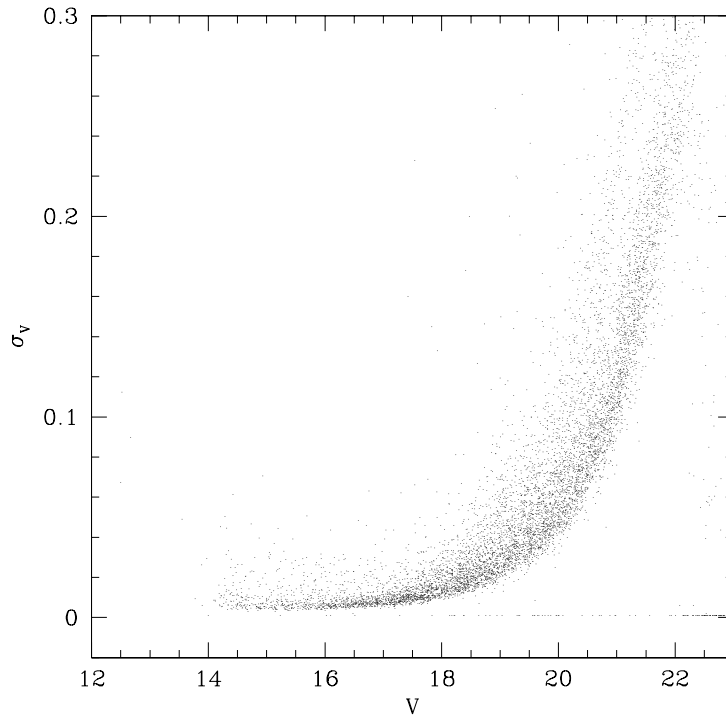


Fig. 4.— The average standard V magnitude errors plotted as a function of V for stars in the comparison field.

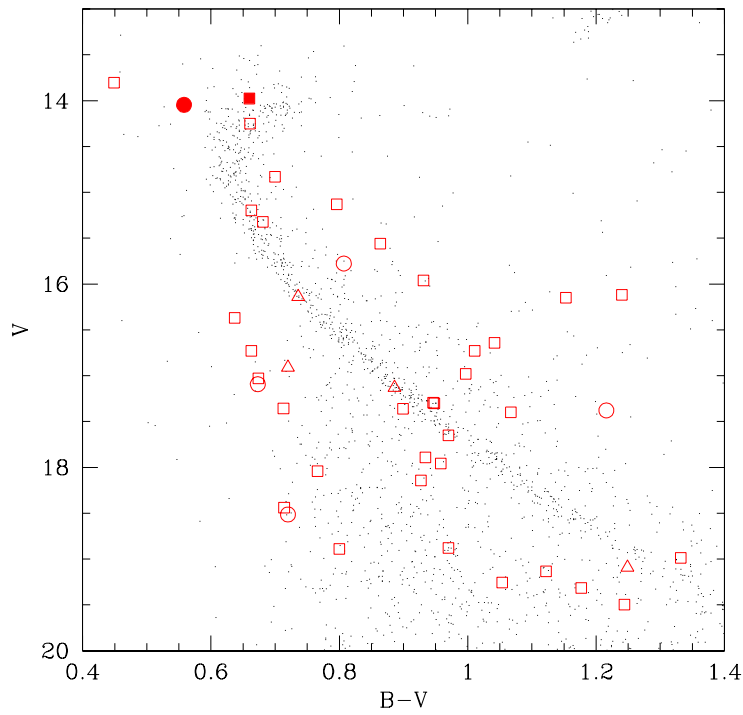


Fig. 5.— The color-magnitude diagram for the variable stars. Eclipsing binaries are marked with squares, pulsating variables with circles and miscellaneous variables with triangles. Solid symbols indicate confirmed cluster members. Stars within a radius of 500 pixels from the cluster center are also plotted.

6. Catalog of variables

In this section we present the light curves of the 45 variables found in the cluster and the comparison fields. The following convention was adopted for the naming of variable stars: letter V for “variable” and the number of the star in the V filter database. For variables found in the comparison field a C is appended to the variable name. Tables 1, 2, 3 list the variables sorted by three categories: eclipsing binaries, pulsating variables and other variables for which we could not obtain a period determination. The light curves of the variables are shown in Figures 6, 7 and 8. The $60'' \times 60''$ finding charts are provided in Figure 10.

6.1. Eclipsing binaries

We have identified 35 eclipsing binaries in both fields, 26 in the cluster field and nine in the comparison field, 26 of them newly discovered. In addition, two of the eclipsing binaries from the cluster field were also identified in the comparison field. In Table 1 we present the parameters for the eclipsing binaries, sorted by period: name, J2000.0 coordinates, period, V_{max} magnitude of the system outside of the eclipse and the average $B - V$ color. Their phased light curves are shown in Figure 6.

Most of the eclipsing binaries have periods shorter than one day and exhibit W UMa type light curves.

The light curves of two variables, V4276 and V6698, show variations similar to those of RS Canum Venaticorum stars. Another variable, V2130, a contact binary, also displays strong assymetry of the light outside of the eclipses: the system achieves maximum brightness between the primary and the secondary eclipse. More observations would be needed to see if and how the light curves evolve with time, to gain insight into the true nature of these systems.

The cataclysmic variable candidate V9, found by Jahn et al. (1995), identified by us as V3283, displays brightness variations outside of the eclipses with an amplitude of 0.03-0.05 mag. on timescales of 1-2 hours, very much like those described in that paper.

Two of our eclipsing binaries have their membership probabilities determined from proper motion analysis by McNamara & Solomon. One of them, V3785 is a cluster member with probability $P = 0.98$ while the other, V9097, is not ($P = 0.0$).

We extracted from our database the light curve for variable V6 found by Jahn et al. (1995). We noticed traces of sinusoidal variability when phased with the published period, but our light curve was too noisy to obtain an independent period determination. We therefore decided not to include this variable into our catalog.

It should be noted that our classification should not be regarded as final. In some cases it was difficult to determine whether a variable is an eclipsing binary or a pulsating variable with

half the period. One example is V820C, which exhibits maxima that may seem too sharp for an eclipsing binary, but was still classified as such because of a slight asymmetry of the minima and its location on the CMD. Information as to the cluster membership would be helpful in many cases. More observations would be needed for some objects, to obtain a better light curve and refine the color determination.

6.2. Pulsating variables

We have found five pulsating variables, three in the cluster field and two in the comparison field, one of them already known. In Table 2 we present the parameters for the pulsating variables, sorted by period: name, J2000.0 coordinates, period, the mean V magnitude and the $\langle B - V \rangle$ color. Their phased light curves are shown in Figure 7.

The variable V3407C is a background RRab Lyrae star. V4805 may also be an RR Lyrae variable. V6736 is most likely a δ Scuti variable and a cluster member with $P = 0.95$ (McNamara & Solomon 1981).

For variables V6669C and V9077 on each night we observed a fall in brightness of about 0.1 mag. We phased them with a period close to 0.5 of a day, but due to an incomplete phase coverage this is not a very reliable estimate.

6.3. Miscellaneous variables

We have identified five other variables, two in the cluster field and three in the comparison field, all of them newly discovered. In table 3 we present the parameters of those variables, sorted by V_{max} magnitude: name, J2000.0 coordinates, the V_{max} magnitude and the $\langle B - V \rangle$ color. Their light curves are shown in Figure 8.

One variable, V5561 is probably a UV Ceti or a BY Dra variable. During five nights of monitoring it underwent an outburst with an amplitude of 4 magnitudes on the second night of observations.

Some of the variables listed here may be periodic, with our observations covering only a part of the period. Due to the short timespan of our observations and few data points obtained on the third night we were able to determine periods shorter than about 2.5 days.

We have detected the variability of the four previously known variables, V11, V13, V14 and V15, found by Jahn et al. (1995). We decided not to include them into our catalog due to the poor quality of the light curves derived from our observations and small amplitudes of variability.

Table 1: ECLIPSING BINARIES IN NGC 7789

Name	<i>RA</i> (2000)	<i>Dec</i> (2000)	<i>P</i> (days)	<i>V_{max}</i>	$\langle B - V \rangle$	Comments
V4947C	23 59 23.01	56 35 51.05	0.2317	16.73	0.66	EW
V2879	23 57 57.25	56 45 48.38	0.2384	19.32	1.18	EW V5
V314C	23 58 46.38	56 46 2.47	0.2651	16.64	1.04	EW
V10021	23 56 18.29	56 34 14.88	0.2731	18.89	0.80	EW
V9860	23 57 25.21	56 34 36.91	0.2789	19.49	1.24	EB
V10461	23 57 10.65	56 33 27.07	0.2790	17.40	1.07	EW
V7790	23 58 12.06	56 38 6.15	0.2907	19.25	1.05	EW
V3983	23 56 38.70	56 43 58.76	0.3063	16.98	1.00	EW
V10517	23 57 34.70	56 33 20.30	0.3228	17.89	0.93	EW
V591C	0 0 39.42	56 45 29.64	0.3354	17.65	0.97	EW
V2130	23 57 49.41	56 46 59.91	0.3375	16.73	1.01	EW V4
V9285	23 56 15.36	56 35 34.72	0.3397	18.44	0.71	EW
V1887	23 58 13.47	56 47 25.70	0.3489	18.99	1.33	EB
V1630C	23 59 40.91	56 43 7.76	0.3499	17.30	0.95	EW
V7874C	23 58 10.64	56 29 33.09	0.3781	18.04	0.77	EW
V3642	23 56 35.86	56 44 30.00	0.3791	18.14	0.93	EW
V820C	23 59 50.81	56 44 55.72	0.3862	15.13	0.80	EW
V662	23 56 50.03	56 49 30.42	0.3957	17.36	0.90	EW
V6698	23 58 37.68	56 39 53.80	0.4044	18.88	0.97	EB
V3255	23 57 24.45	56 45 13.00	0.4567	15.96	0.93	EW V7
V547	23 56 44.55	56 49 44.23	0.4902	17.96	0.96	EB
V1524C	23 59 33.48	56 43 23.88	0.5134	17.29	0.95	EW?
V1176	23 56 56.38	56 48 34.79	0.7061	17.36	0.71	EA
V3641	23 57 33.45	56 44 32.95	0.7164	14.83	0.70	EB V2
V3283	23 57 0.19	56 45 8.47	0.7806	19.13	1.12	EA V9
V4276	23 57 25.68	56 43 33.22	0.8481	15.20	0.66	EB V8
V5979	23 57 39.45	56 41 0.07	1.0434	15.32	0.68	EA V3
V10289	23 56 9.06	56 33 42.92	1.0896	15.56	0.86	EA
V5106	23 57 9.92	56 42 18.08	1.1614	14.25	0.66	EW V1
V3785	23 56 32.15	56 44 17.60	1.2007	13.98	0.66	EA
V7798C	23 59 21.52	56 29 48.39	1.6617	17.03	0.67	EA
V7572	23 56 50.81	56 38 26.21	1.7327	16.12	1.24	EA V12
V9097	23 57 38.60	56 35 58.04	2.1077	13.80	0.45	EA
V10231	23 57 44.85	56 33 55.63	2.3362	16.15	1.15	EW
V3346C	23 59 3.73	56 39 17.32	3.0314	16.37	0.64	EA

7. Cluster membership of the contact binaries

In an attempt to assess the cluster membership of the contact binaries we have applied the absolute magnitude calibration established by Rucinski & Duerbeck (1997) to calculate their M_V . The adopted calibration expresses M_V as a function of the period and the unreddened color $(B - V)_0$:

$$M_V = -4.44 \cdot \log P + 3.02 \cdot (B - V)_0 + 0.12 \quad (1)$$

We assumed a uniform value of reddening $E(B - V) = 0.24$ mag. across the face of the cluster. The weighted mean deviation for the stars used to derive the calibration was $\sigma = 0.22$ mag. The calibration has not been applied to V10231, tentatively classified as a contact binary, due to a period outside of the validity range for the calibration. The apparent distance modulus was calculated for each system as the difference between its V_{max} and M_V^{cal} magnitudes. Figure 9 shows the period versus apparent distance modulus diagram for the contact binaries found in both the cluster and the comparison field. The variable V5106 with an apparent distance modulus of 13.147 mag. is not shown in the plot, due to an outlying period.

Five systems, V10461, V3983, V2130, V3255 and V4947C seem to be cluster members, with computed distance moduli within about ± 0.2 of the cluster’s distance modulus. There seem to be no other variables within 0.7 mag. in front of or behind the cluster. Only two variables, V314C and V820C are foreground systems, while the rest of the W-UMa type systems are located behind the cluster.

8. Conclusions

Our search for variable stars in the open cluster NGC 7789 has resulted in the discovery of 45 variables: 35 eclipsing binaries, five pulsating variables and five miscellaneous variables for which we could not determine a period from our short span observations. Among those we have found four interesting candidates for in-depth photometric and spectroscopic studies: two RS CVn eclipsing binaries, V4276 and V6698, one possible cataclysmic variable, V3283, and one system of an unclear nature, V2130.

Table 2: PULSATING VARIABLES IN NGC 7789

Name	$RA(2000)$	$Dec(2000)$	P (days)	$\langle V \rangle$	$\langle B - V \rangle$	Comments
V6736	23 57 30.93	56 39 49.31	0.0868	14.05	0.56	δ Sct V10
V6669C	23 58 22.86	56 32 9.90	0.4940	17.38	1.22	
V9077	23 57 58.79	56 36 0.30	0.4960	17.09	0.67	
V3407C	0 0 6.64	56 39 12.11	0.6437	18.51	0.72	RR Lyr
V4805	23 57 53.72	56 42 44.52	0.7334	15.78	0.81	RR Lyr

Only about twice as many variables were found in the field centered on the cluster as in the comparison field (31 as opposed to 14). This implies that objects not associated physically with the cluster may have a significant share in the total number of variables found in the cluster field, as well as in other globular and open clusters observed on a dense background/foreground of disk stars.

We would like to thank Krzysztof Z. Stanek for his error scaling, database manipulation and period finding programs and Grzegorz Pojmański for *lc* - the light curve analysis utility, incorporating the analysis of variance algorithm. BJM was supported by the polish KBN grant 2P03D01416 to Grzegorz Pojmański. JK was supported by the polish KBN grant 2P03D00317 and by the NSF grant AST-9528096 to Bohdan Paczynski.

Table 3: MISCELLANEOUS VARIABLES IN NGC 7789

Name	<i>RA</i> (2000)	<i>Dec</i> (2000)	V_{max}	$\langle B - V \rangle$	Comments
V545	23 57 29.98	56 49 46.57	16.14	0.74	
V8064C	23 59 25.18	56 29 10.92	16.91	0.72	
V6744C	23 58 18.03	56 31 58.74	17.13	0.89	
V7717C	23 58 25.12	56 29 55.66	19.09	1.25	
V5561	23 56 8.30	56 41 34.02	19.83	...	UV Ceti

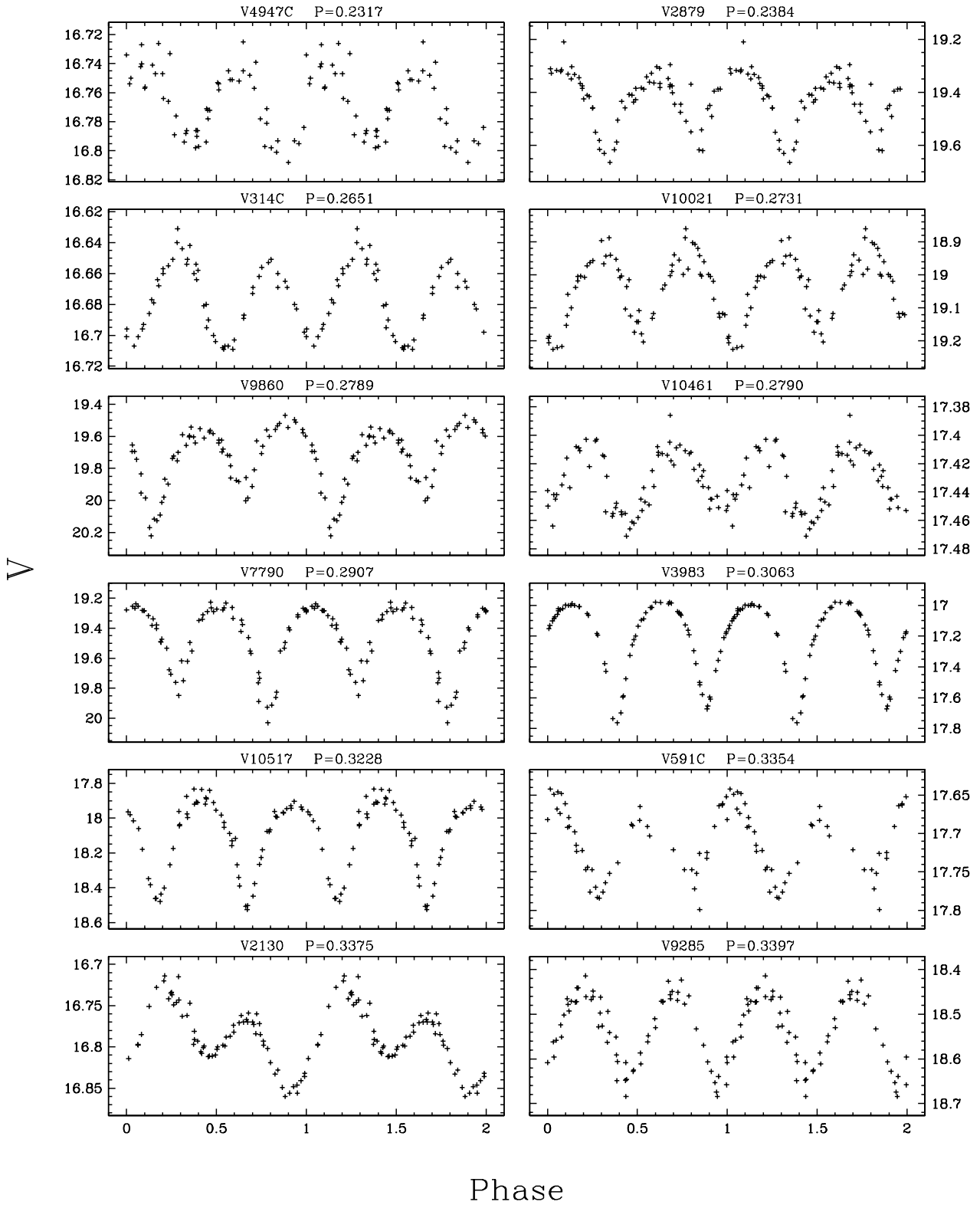


Fig. 6.— Phased V filter light curves of the eclipsing binaries.

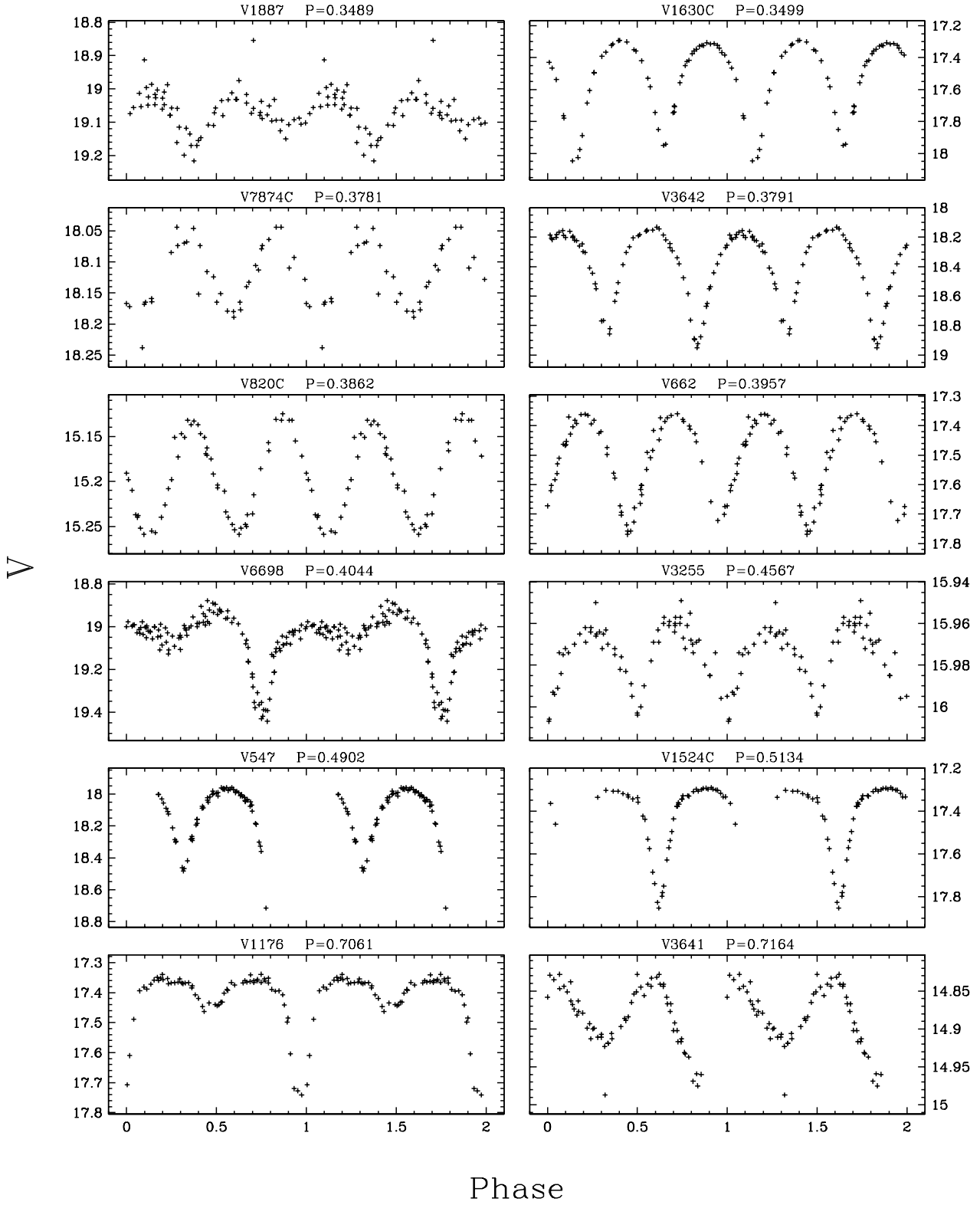


Fig. 6.— Continued.

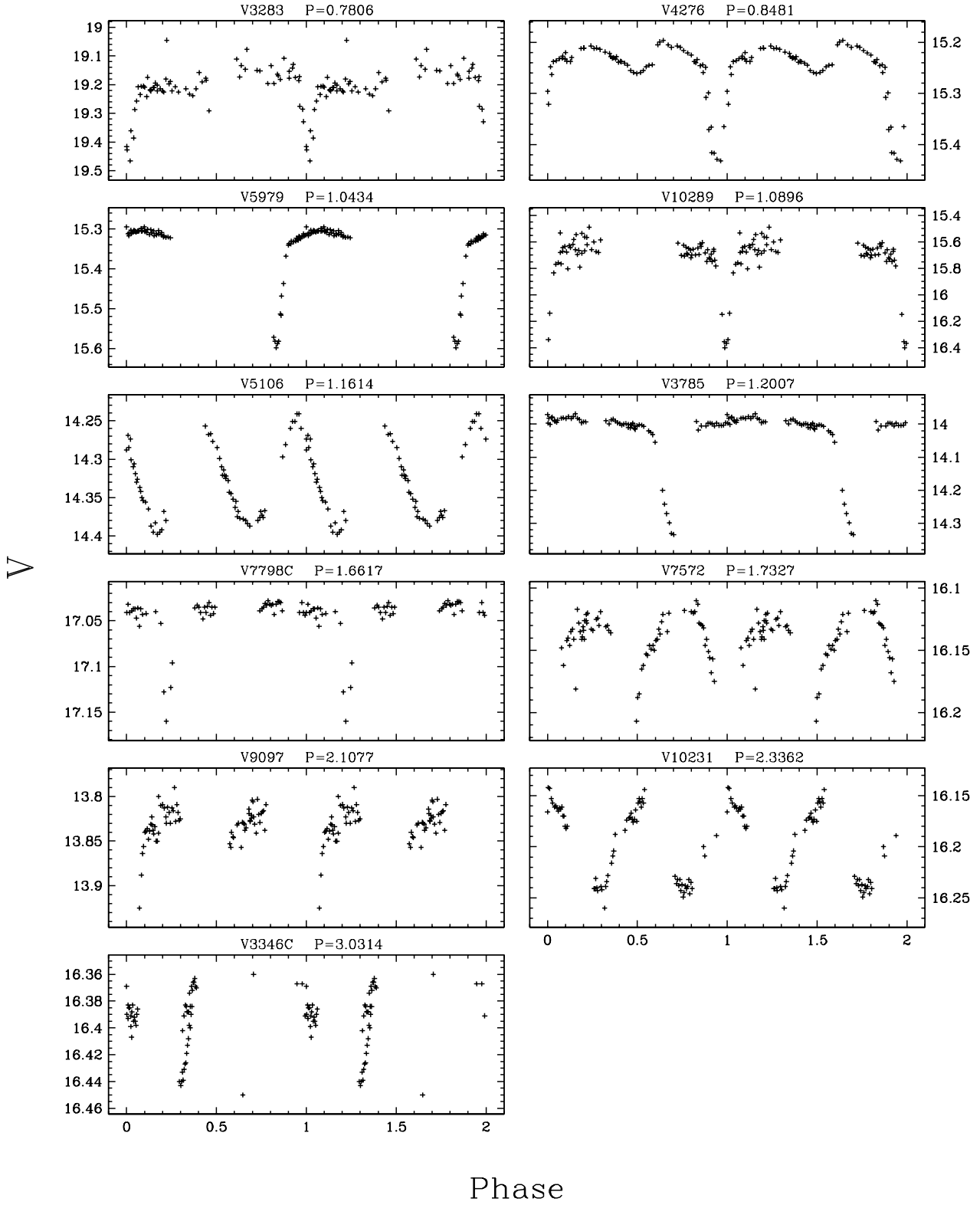


Fig. 6.— Continued.

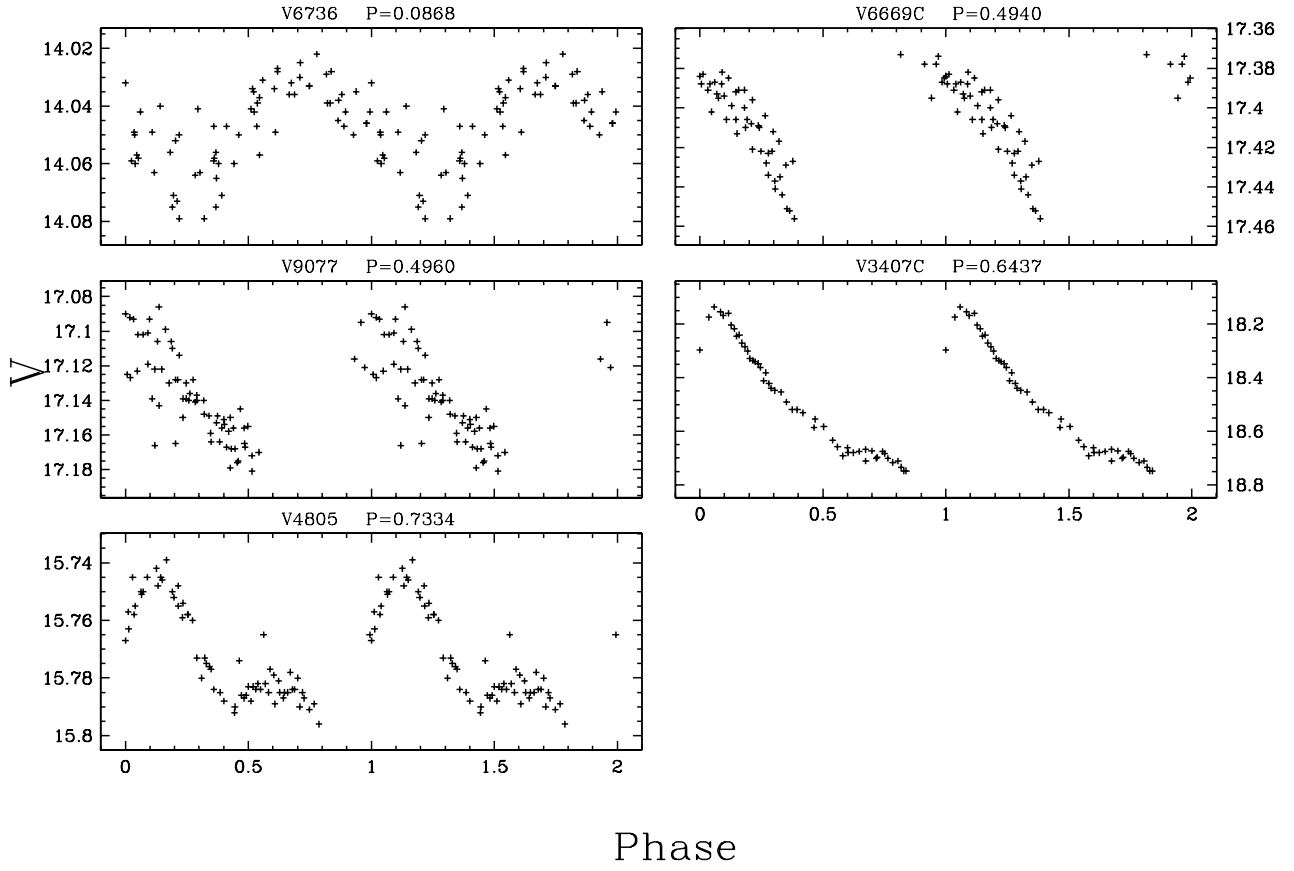


Fig. 7.— Phased V filter light curves of the pulsating variables.

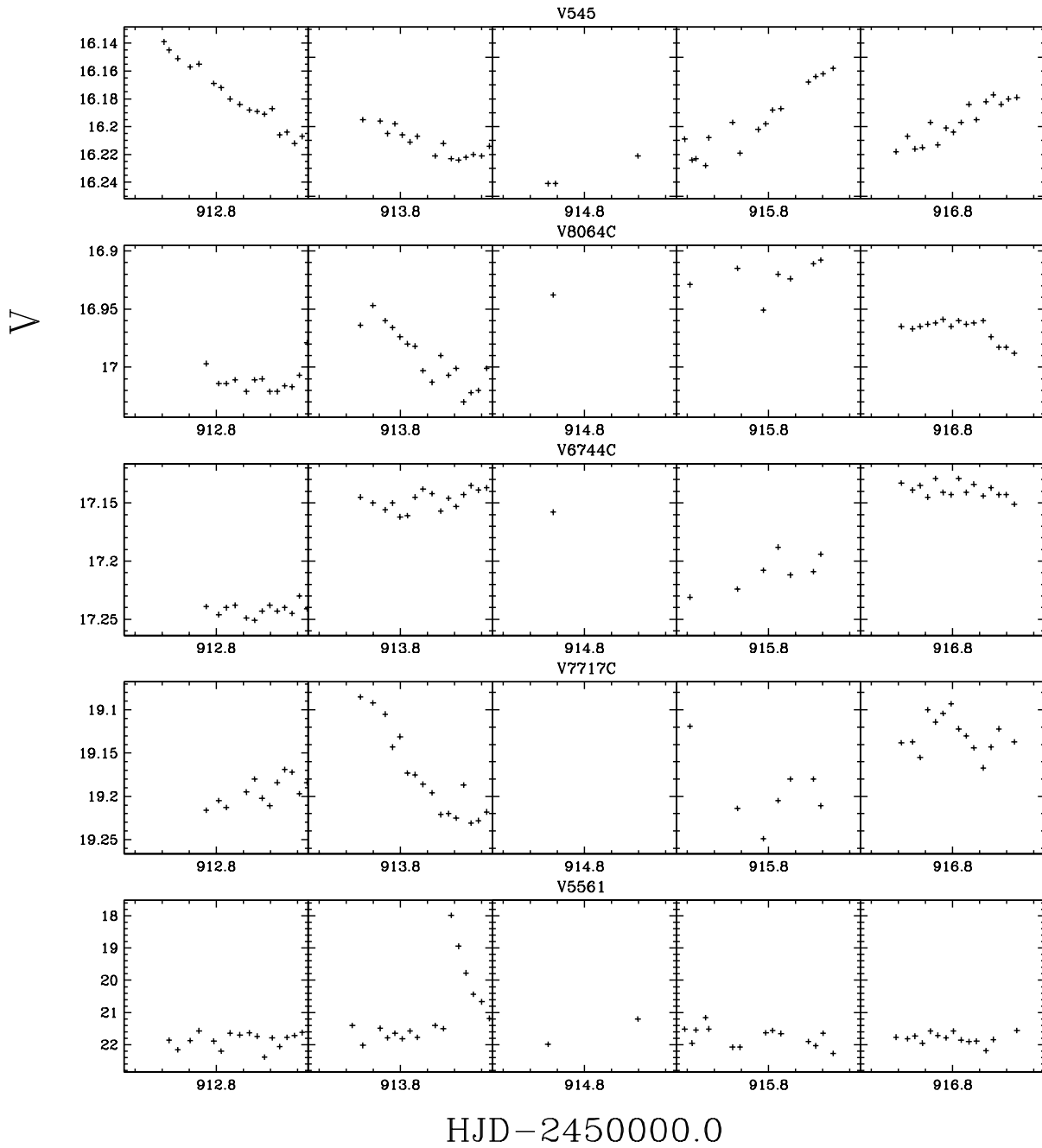


Fig. 8.— The V filter light curves of the miscellaneous variables.

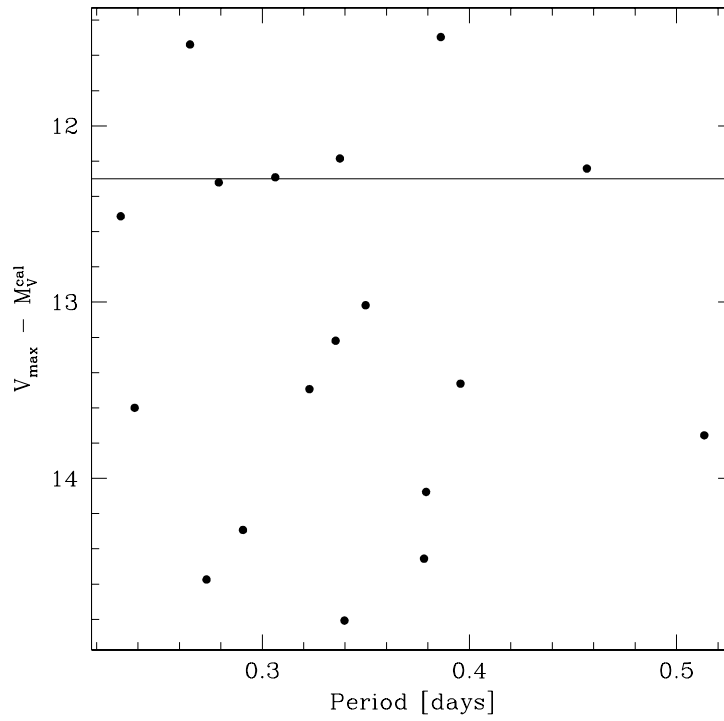


Fig. 9.— The period versus apparent distance modulus diagram for the contact binaries found in both the cluster and the comparison field. The variable V5106 with an apparent distance modulus of 13.147 mag. is not shown in the plot, due to an outlying period.

REFERENCES

- Burbridge, E. M., Sandage, A., 1958, ApJ, 128, 174
- Gim, M., VandenBerg, D. A., Stetson, P. B., Hesser, J. E., Zurek, D. R., 1998, PASP, 110, 1318
- Jahn, K., Kaluzny, J., Ruciński, S. M. 1995, A&A, 295, 101
- Laffer, J., & Kinman, T. D. 1965, ApJS, 11, 216
- Landolt, A., 1992, AJ, 104, 340
- Kaluzny, J., Stanek, K. Z., Krockenberger, M., Sasselov, D. D., Tonry, J. L., & Mateo, M. 1998, AJ, 115, 1016
- McNamara, B. J. & Solomon S., 1981, A&AS, 43, 337
- Monet, D., et al. 1996, USNO-SA2.0, (U.S. Naval Observatory, Washington DC)
- Rucinski, S. M., Duerbeck, H. W., 1997, PASP, 109, 1340
- Stetson, P. B. 1996, PASP, 108, 851
- Stetson, P. B. 1997, PASP, 99, 191
- Schwarzenberg-Czerny, A., 1989, MNRAS 253, 198

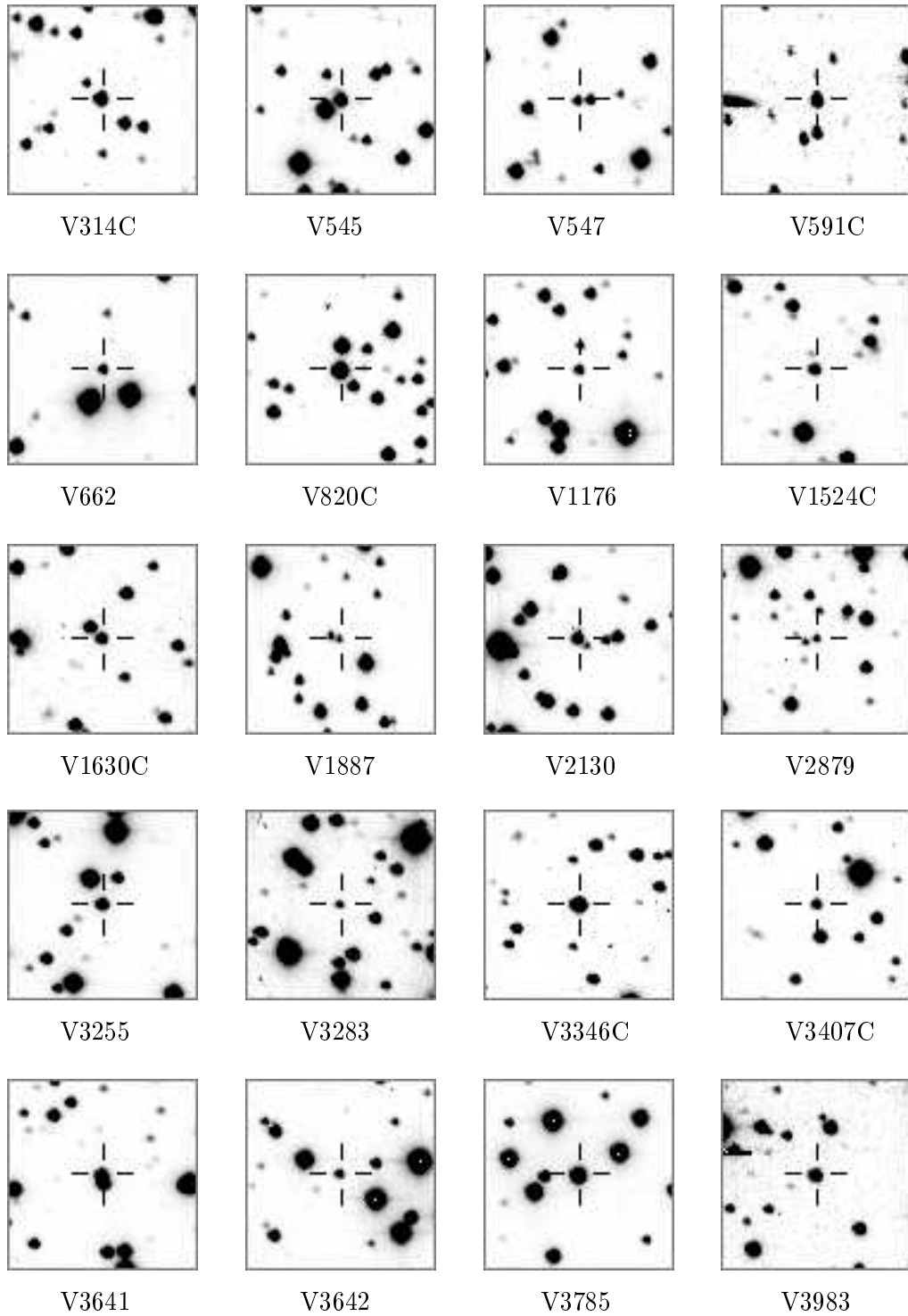


Fig. 10.— Finding charts for the cluster and comparison field variables, sorted by ID. North is up and east is to the left.

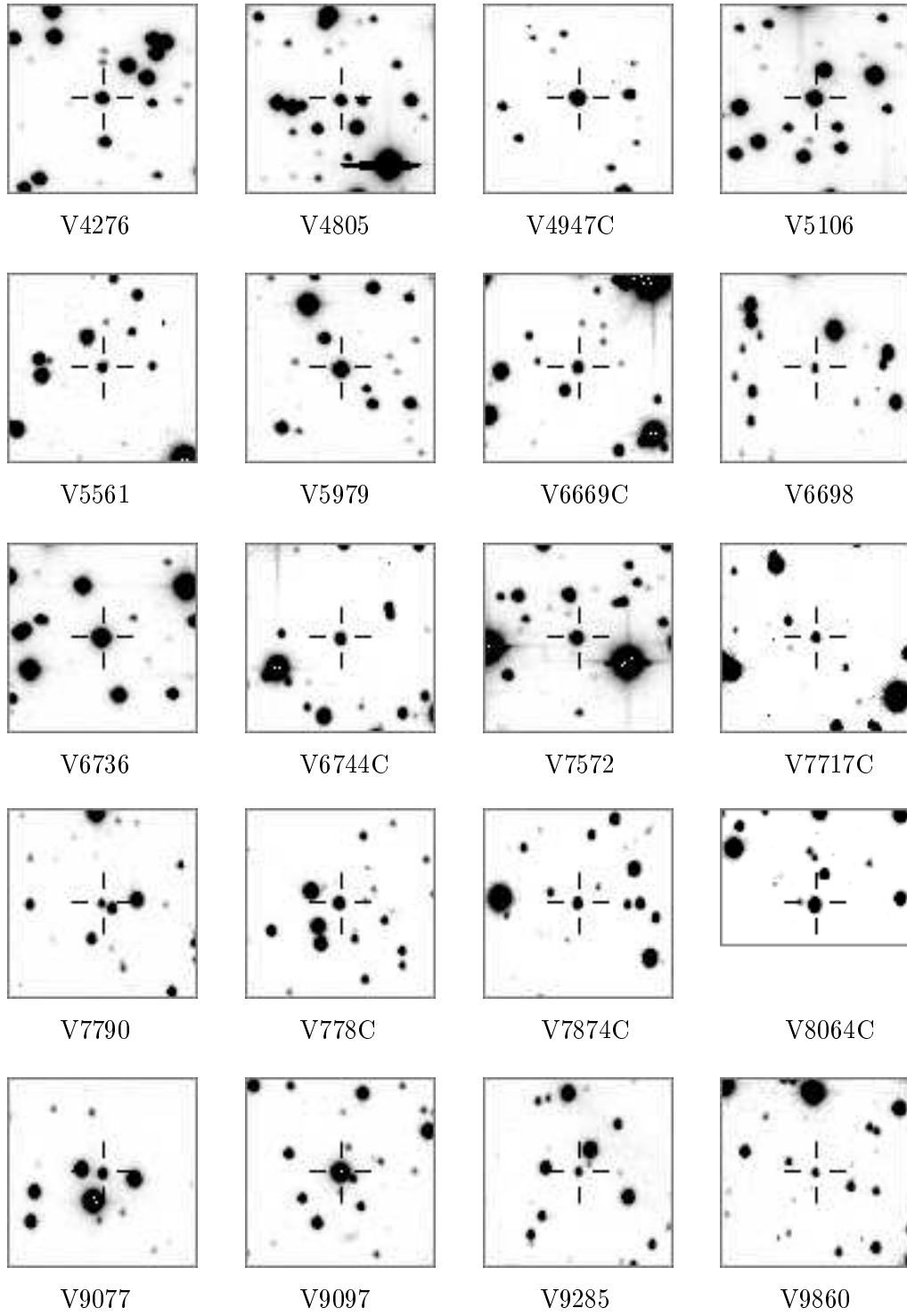
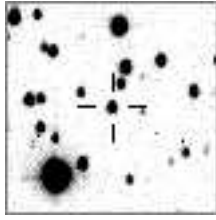
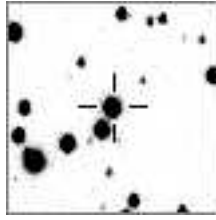


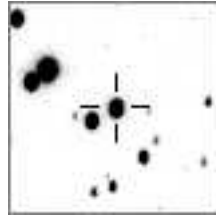
Fig. 10.— Continued.



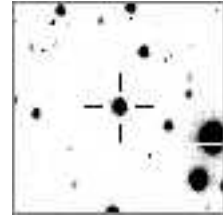
V10021



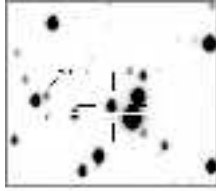
V10231



V10289



V10461



V10517

Fig. 10.— Continued.